# Ice-shelf collapse from subsurface warming as a trigger for Heinrich events

Shaun A. Marcott[a,1], Peter U. Clark[a], Laurie Padman[b], Gary P. Klinkhammer[c], Scott R. Springer[d], Zhengyu Liu[e], Bette L. Otto-Bliesner[f], Anders E. Carlson[e,g], Andy Ungerer[c], June Padman[c], Feng He[e], Jun Cheng[h], and Andreas Schmittner[c]

[a]Department of Geosciences, Oregon State University, Corvallis, OR 97331; [b]Earth and Space Research, 3350 SW Cascade Avenue, Corvallis, OR 97333; [c]College of Oceanic and Atmospheric Sciences, Oregon State University, Corvallis, OR 97331; [d]Earth and Space Research, 2101 Fourth Avenue, Suite 1310, Seattle, WA 98121; [e]Center for Climatic Research and Department of Atmospheric and Oceanic Sciences, University of Wisconsin, Madison, WI 53706; [f]Climate and Global Dynamics Division, National Center for Atmospheric Research, Boulder, CO 80307; [g]Department of Geoscience, University of Wisconsin, Madison, WI 53706; and [h]Key Laboratory of Meteorological Disaster, Nanjing University of Information Science and Technology, Nanjing, 210044, China

Edited by Mark H. Thiemens, University of California San Diego, La Jolla, CA, and approved June 30, 2011 (received for review March 25, 2011)

**Episodic iceberg-discharge events from the Hudson Strait Ice Stream (HSIS) of the Laurentide Ice Sheet, referred to as Heinrich events, are commonly attributed to internal ice-sheet instabilities, but their systematic occurrence at the culmination of a large reduction in the Atlantic meridional overturning circulation (AMOC) indicates a climate control. We report Mg/Ca data on benthic foraminifera from an intermediate-depth site in the northwest Atlantic and results from a climate-model simulation that reveal basin-wide subsurface warming at the same time as large reductions in the AMOC, with temperature increasing by approximately 2 °C over a 1–2 kyr interval prior to a Heinrich event. In simulations with an ocean model coupled to a thermodynamically active ice shelf, the increase in subsurface temperature increases basal melt rate under an ice shelf fronting the HSIS by a factor of approximately 6. By analogy with recent observations in Antarctica, the resulting ice-shelf loss and attendant HSIS acceleration would produce a Heinrich event.**

paleoceanography | paleoclimatology | abrupt climate change

Heinrich events represent the episodic discharge of icebergs from the Hudson Strait Ice Stream (HSIS) of the Laurentide Ice Sheet to the North Atlantic Ocean during late-Pleistocene glaciations (1). Although commonly attributed to internal ice-sheet instabilities (2), their occurrence at the culmination of a large reduction in the Atlantic meridional ocean circulation (AMOC) suggests a possible trigger by climate (3, 4). Models suggest that ocean responses to an AMOC reduction might destabilize the HSIS grounding line and trigger Heinrich events either through dynamic and steric sea-level rise or warming of intermediate-depth (hereafter subsurface) waters causing destabilization of ice shelves and attendant HSIS surging (4–6). Grounding lines, however, are thought to be stable to the decimeter-scale sea-level rise associated with a reduced AMOC (7). Moreover, evidence for subsurface warming remains widely debated (8–10), and the relationship between ocean temperature and total ice-shelf mass loss from basal melting is sensitive to the geometry and ocean setting of the specific ice shelf being considered (11).

Our study is based on core EW9302-2JPC (1,251 m, 48°47.70′ N, 45°05.09′W) which, according to climate-model simulations, is at a depth and latitude that is ideal for monitoring subsurface warming associated with a reduction in the AMOC (Fig. 1) (4, 12). Previous work on this core identified ice-rafted detrital carbonate layers that represent Heinrich events (Fig. 2*A*), with associated changes in benthic faunas and the $\delta^{18}$O of their carbonate tests that suggested intrusions of a relatively warm water mass coincident with the events (8). However, because the temperature transfer function for the benthic faunas is unknown, and ice-volume and hydrographic changes can mask the temperature signal in the $\delta^{18}$O of calcite, the inferred temperature changes remain poorly constrained.

To further evaluate variability in bottom water temperature (BWT) at this site, we measured Mg/Ca in benthic foraminiferal calcite associated with the four Heinrich events (H1, H3, H5a, and H6) for which sufficient numbers of foraminifera existed in this core. Considering analytical and calibration uncertainties, we calculate an error of 1.3 °C for our Mg/Ca-derived BWT reconstructions. Recent work suggests that the $[CO_3^{2-}]$ ion may also affect Mg/Ca in some benthic foraminifera at temperatures below approximately 3 °C, where the carbonate ion saturation ($\Delta[CO_3^{2-}]$) decreases rapidly, and at low saturation levels (13). We used CO2SYS (14) to calculate modern $\Delta[CO_3^{2-}]$ at our site based on values of temperature, pressure, salinity, total alkalinity, total $CO_2$, phosphate, and silicate retrieved from the World Ocean Circulation Experiment (WOCE) database (15). The corresponding value (approximately 55 mol/kg) suggests that the site is very weakly affected by the $[CO_3^{2-}]$ effect today (13). During the last glacial period, the deep Atlantic Ocean was less saturated in $[CO_3^{2-}]$, decreasing by approximately 20 $\mu$mol/kg due to the intrusion of cold, undersaturated Antarctic Bottom Water (16). At intermediate-water depths (1–2 km) such as for our site, however, the glacial North Atlantic was approximately 20–30 $\mu$mol/kg higher in $[CO_3^{2-}]$ than present and Holocene values (16), suggesting that our measured Mg/Ca values were not influenced by past $\Delta[CO_3^{2-}]$.

## Results

Two independent temperature proxies support our Mg/Ca-derived BWTs. First, our reconstructed BWT at approximately 19 ka of $0 \pm 1.3$ °C agrees at 1σ with a Last Glacial Maximum temperature of $-1.2 \pm 0.2$ °C reconstructed from pore fluids at site 981 on the Feni Drift (2,184 m; 55°29′N, 14°39′W) (17). Second, the amplitude and structure of the BWT change during the last deglaciation is in excellent agreement with the temperature change derived from the ice-volume corrected $\delta^{18}$O ($\delta^{18}O_{IVC}$) measured on benthic fauna from this core assuming a temperature-dependent fractionation of 0.25‰ °C$^{-1}$ for calcite (18) (*SI Text*) (Fig. 2*B*).

The Mg/Ca data from EW9302-2JPC identify several systematic BWT changes that occurred in association with each of the four Heinrich ice rafted debris layers for which we have sufficient data (Fig. 2*B*) (1). Temperatures gradually increased prior to the start of each Heinrich layer, with the start of the warming begin-

Author contributions: P.U.C. designed research; S.A.M., L.P., S.R.S., Z.L., and B.L.O.-B. performed research; S.A.M., P.U.C., L.P., G.P.K., A.E.C., A.U., J.P., F.H., J.C., and A.S. analyzed data; and S.A.M., P.U.C., and L.P. wrote the paper.

The authors declare no conflict of interest.

This article is a PNAS Direct Submission.

[1]To whom correspondence should be addressed. E-mail: marcotts@geo.oregonstate.edu.

This article contains supporting information online at www.pnas.org/lookup/suppl/doi:10.1073/pnas.1104772108/-/DCSupplemental.

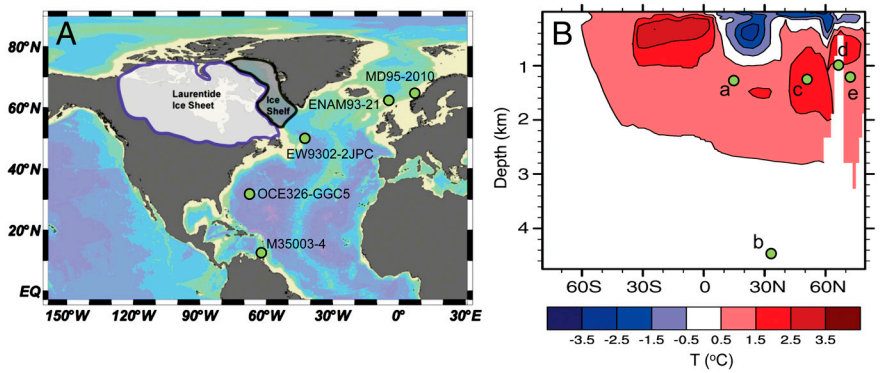


**Fig. 1.** (*A*) Location of core sites with records discussed in text (red dots). Also shown is extent of ice shelf derived from the Hudson Strait Ice Stream as reconstructed in ref. 31. (*B*) Zonal mean temperature anomaly in the Atlantic basin for a strongly reduced (approximately 4 Sv) versus active (approximately 13 Sv) AMOC (12). Location of core sites also shown: site a is core M35003-4, site b is core OCE326-GGC5, site c is core EW9302-2JPC, site d is core ENAM93-21, and site e is core MD95-2010.

ning approximately 1–2 kyr before each Heinrich event on our time scale. This early warming is replicated by the $\delta^{18}O_{IVC}$ (temperature) record associated with H1 (2). The warming trend prior to each Heinrich layer is consistently associated with a temperature oscillation of 3–4 °C (3). Each temperature oscillation occurs around a mean value that is close to the present BWT of approximately 3.4 °C and reaches a maximum BWT of 5–7 °C during the Heinrich layer.

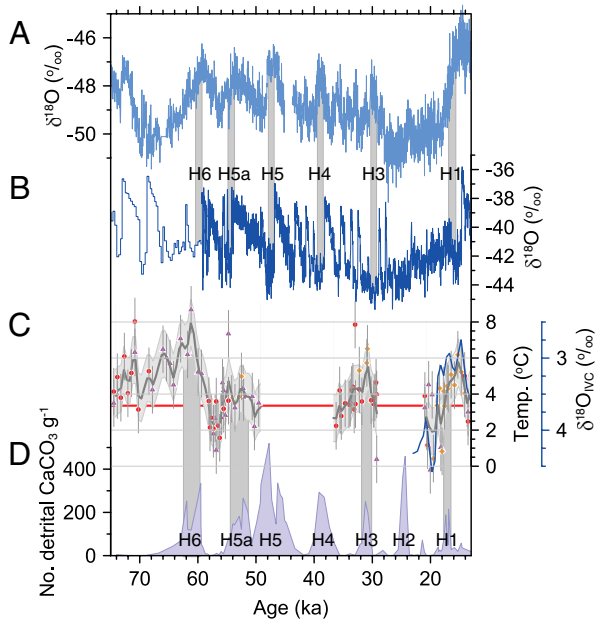


**Fig. 2.** (*A*) $\delta^{18}O$ record from Antarctic EPICA (European Project for Ice Coring in Antarctica) Dronning Maud Land ice core (37) on revised age model (38). (*B*) $\delta^{18}O$ record from the North Greenland Ice Core Project ice core (39) on revised age model (38) (<60 ka) and from Greenland Ice Core Project 2 ice core (>60 ka) on published age model (40). (*C*) Mg/Ca-derived bottom water temperatures for core EW9302-2JPC (1,251 m, 48°47.70′N, 45°05.09′W). Orange diamonds are measurements on *C. spp*, purple triangles are on *C. lobulatus*, and red circles are on *M. barleeanum*. In order to filter the higher frequency signal to better evaluate the longer-term temperature changes, we linearly interpolated our data to a 10-yr interval and then applied a 500-yr Gaussian filter to derive the time series shown (thick gray line), with a 1.3 °C error based on analytical uncertainty. Also shown is the ice-volume corrected benthic $\delta^{18}O$ ($\delta^{18}O_{IVC}$) record from this core (blue line) during the last deglaciation (*SI Text*). (*D*) Number of ice-rafted detrital $CaCO_3$ grains $g^{-1}$ of sediment in core EW9302-2JPC, with increases in these grains identifying Heinrich layers 1 through 6 (*SI Text*). Vertical gray bars represent timing of Heinrich events on the independent ice core (*A* and *B*) and EW9302-2JPC core (*C* and *D*) chronologies.

A number of proxy records show that the AMOC began to decrease 1–2 kyr prior to Heinrich events (3, 19–22); this decline has been attributed to a climatically induced increase in freshwater fluxes from Northern Hemisphere ice sheets (4, 23). Model simulations indicate that, without an active AMOC and associated cooling of the ocean interior by convection, continued downward mixing of heat at low latitudes warms subsurface waters to a depth of approximately 2,500 m. Some of the heat accumulated in the subsurface is transported poleward, causing a temperature inversion in the northern North Atlantic (Fig. 1*B*) (4, 5, 12). We use results from a simulation with the National Center for Atmospheric Research Community Climate System Model version 3 (NCAR CCSM3) (12) to evaluate the transient response of the BWT at our core site to a reduction in the AMOC during the last deglaciation. Initial reduction in the AMOC occurs in response to increased freshwater fluxes to the North Atlantic associated with onset of deglaciation from the last glacial maximum at approximately 19 ka (Fig. 3*A*) (12, 23). Here we find that the simulated BWT anomaly at our core site caused by the change in the AMOC is in good agreement with our Mg/Ca-derived record, with temperature increasing by approximately 2 °C prior to H1, followed by cooling induced by the resumption of the AMOC at the start of the Bølling interstadial approximately 14.6 ka (Fig. 3*C*).

Although similar subsurface warming preceding H1 has been inferred in the subtropical (24) and high-latitude (25, 26) North Atlantic from changes in benthic foraminifera $\delta^{18}O$, the $\delta^{18}O$ changes in the Nordic Seas have alternatively been interpreted as recording increased brine formation beneath expanded sea ice (9, 10) and thus are largely independent of temperature. Our previously undescribed Mg/Ca measurements on *Cibicidoides spp.* ($N = 1$), *Cibicidoides lobulatus* ($N = 3$), and *Melonis barleeanum* ($N = 16$) for a core from the Nordic Seas (MD95-2010, 1,226-m depth) (Fig. 1*B*) demonstrate that the 1.5 per mil $\delta^{18}O_{IVC}$ signal at this site can be explained by approximately 6 °C of warming (Fig. 4*A*), thus supporting subsurface warming rather than brine formation as the cause of the large $\delta^{18}O_{IVC}$ signal. Changes in temperature simulated by the CCSM3 model further suggest that the $\delta^{18}O_{IVC}$ signal at this and other North Atlantic sites represents a dominant temperature control reflecting basin-wide subsurface warming (Fig. 4). The model also simulated small changes in salinity at intermediate depths as freshwater added to the surface was convected downward through the Labrador Sea in the subpolar gyre, suggesting that the associated advection of light $\delta^{18}O$ water may account for some small fraction of the $\delta^{18}O_{IVC}$ signal (Fig. 4) (*SI Text*).

Our Mg/Ca data also suggest a similar phasing between earlier changes in the AMOC, subsurface temperatures, and Heinrich events during marine isotope stage 3 (60–26 ka). In particular, correlation of marine records with synchronized Greenland

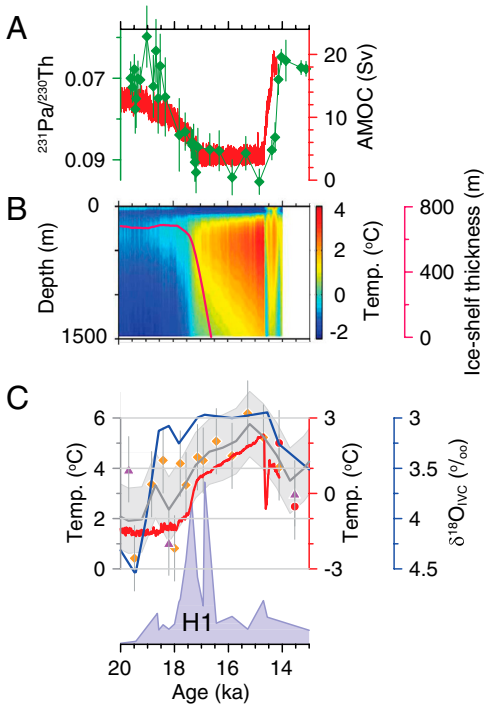


**Fig. 3.** (*A*) Comparison between the $^{231}Pa/^{230}Th$ record from the Bermuda Rise (core OCE326-GGC5), a proxy of AMOC strength (19), and strength of the maximum AMOC transport simulated by the NCAR CCSM3 (12) during the last deglaciation. (*B*) Evolution of temperature as a function of time and depth simulated by the NCAR CCSM3 at the location of core EW9302-2JPC. Also shown is the evolution of computed changes ice-shelf thickness (red line) in response to the temperature evolution (*SI Text*). (*C*) Mg/Ca-derived bottom water temperatures for core EW9302-2JPC. Orange diamonds are measurements on *C. spp.*, purple triangles are on *C. lobulatus*, and red circles are on *M. barleeanum*. In order to filter the higher frequency signal to better evaluate the longer-term temperature changes, we linearly interpolated our data to a 10-yr interval and then applied a 500-yr Gaussian filter to derive the time series shown (thick gray line), with a 1.3 °C error based on analytical uncertainty. Also shown is the ice-volume corrected benthic $\delta^{18}O$ ($\delta^{18}O_{IVC}$) record from this core (blue line) and the temperature for the core site simulated by the NCAR CCSM3 (red line). Ice-rafted detrital $CaCO_3$ record of Heinrich event 1 from the core shown by light blue fill pattern.

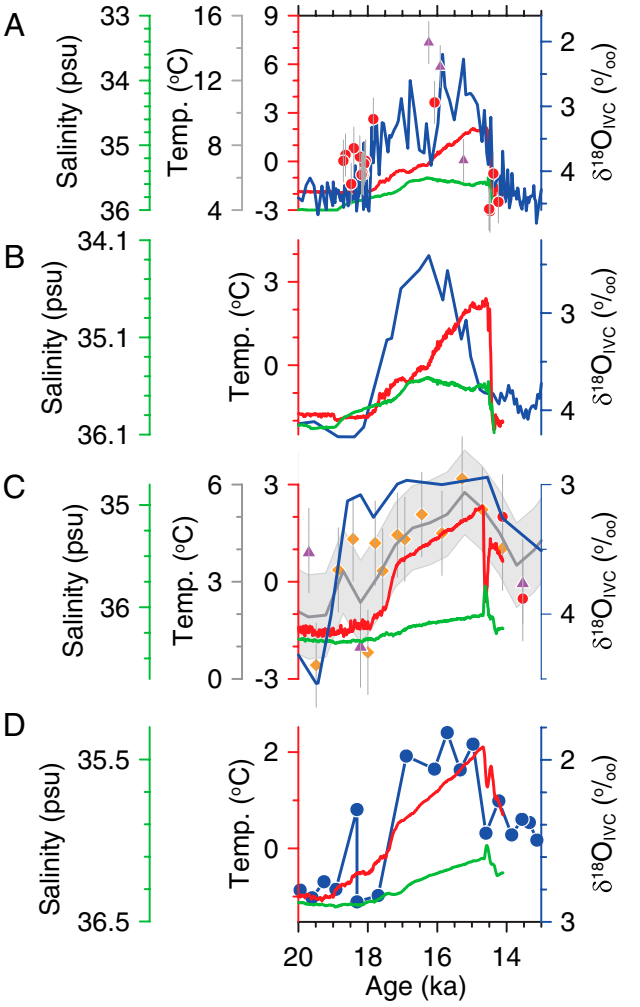


**Fig. 4.** Comparison of $\delta^{18}O_{IVC}$ records from a subtropical North Atlantic site and two sites from the Nordic Seas (Fig. 1) with changes in temperature and salinity simulated by the CCSM3 model at these sites in response to the decrease in the AMOC shown in Fig. 3*A*. The temperature scale for each plot is equivalent to the associated $\delta^{18}O_{IVC}$ scale assuming a temperature-dependent fractionation of 0.25‰ °$C^{-1}$ for calcite (18). (*A*) Ice-volume corrected benthic $\delta^{18}O$ ($\delta^{18}O_{IVC}$) record from core MD95-2010 (1,226 m depth; 66°41.05′ N, 04°33.97′ E) during the last deglaciation. Also shown is the temperature (red line) and salinity (green line) for the core site simulated by the NCAR CCSM3, and our new Mg/Ca-derived bottom water temperatures, where purple triangles are on *C. lobulatus* and red circles are on *M. barleeanum*. (*B*) As in *A*, but for core ENAM93-21 (1,020 m depth; 66°44.3′ N, 03°59.92′ E) (25). (*C*) Mg/Ca-derived bottom water temperatures for core EW9302-2JPC. Orange diamonds are measurements on *C. spp.*, purple triangles are on *C. lobulatus*, and red circles are on *M. barleeanum*, with a 3-point weighted average (blue line). Also shown is the temperature (red line) and salinity (green line) for the core site simulated by the NCAR CCSM3. (*D*) As in *A*, but for core M35003-4 (1,299 m depth; 12°05′N, 61°15′W) (41).

and Antarctica ice-core temperature records shows that Heinrich events during this interval occurred only when Greenland was at its coldest and Antarctica was at its warmest (Fig. 2 *C* and *D*) (27, 28), which is the maximum expression of a strong reduction in the AMOC and its attendant meridional ocean heat transport (29). These changes in the AMOC are documented by a variety of proxy records that show a gradual AMOC reduction prior to and the near-complete replacement of North Atlantic Intermediate Water with Antarctic Bottom Water in the North Atlantic basin at the times of Heinrich events (3, 22, 30). The 1- to 2-kyr interval of gradual subsurface warming suggested by our Mg/Ca data that peak at the same time as H3, H5a, and H6 (Fig. 2*A*) is thus consistent with a response to a maximum reduction in the AMOC at these times as well.

Because of the complex ocean-ice processes that exist beneath ice shelves (11), the effect of the open-ocean subsurface warming documented here on the stability of an ice shelf fronting the HSIS is unclear. We apply a high-resolution ocean model coupled to a nonevolving but thermodynamically active ice shelf (*SI Text*) to explore the sensitivity of basal melt rate to subsurface warming for a specified ice shelf filling Baffin Bay and the Labrador Sea (31). Initial model hydrography is derived from the CCSM3 simulation of the last deglaciation (*SI Text*) (12). We refer to an active AMOC, with cold subsurface temperatures, as the "cold state," corresponding to model years 19.5–19.0 ka, and an inactive AMOC, with warm subsurface temperatures, as the "warm state," corresponding to model years 17.0–16.5 ka.

For the cold state, we find that the shelf-averaged basal melt rate is 0.17 $ma^{-1}$, with the integrated volume loss from the ice shelf by basal melt being approximately 10% of the estimated flux of approximately 660 $km^3\,a^{-1}$ across the HSIS grounding line (31). For the warm state, the averaged basal melt rate is 1.03 $m\,a^{-1}$. We also performed three additional intervening simulations with our regional model, for a total of five spanning the interval from 19.5 to 16.5 ka, which allows us to derive the rela-

tion between ocean temperature $T_i$ at the typical depth of the ice-shelf base (400–800 m), and shelf-averaged melt rate $M_{av} = 0.54 + 0.34.T_i$ (m $a^{-1}$). Based on the simulated temperature evolution for water depths of 400–800 m, our computed time history of ice-shelf thinning in response to the warming of intermediate-depth waters indicates an approximate 1,000-year time scale for collapse of the ice shelf (red curve in Fig. 3*B*), although based on modern analogs, it is likely that the ice shelf would collapse before it thinned to zero; we thus expect that our estimate of this time scale is a maximum. Additional factors (rate of grounding line migration and calving rate) may modulate this response, but are unlikely to significantly change the time scale (*SI Text*). The model also indicates that maximum melt rates along the deep grounding line of the HSIS increased sixfold, from approximately 6 m $a^{-1}$ to 35–40 m $a^{-1}$, comparable to estimates from empirical models based on modern observations of grounding line melt rates (32). By analogy with recent studies of Antarctic ice shelves and buttressed ice streams (33), more rapid grounding line thinning would accelerate the HSIS outflow prior to ice-shelf collapse.

## Conclusions

Our data and model results indicate that basin-wide subsurface warming occurred in the North Atlantic in response to a reduction in the AMOC prior to Heinrich events and that Heinrich events did not occur until the AMOC was at its weakest and subsurface temperatures were near their maximum values. We also find that the open-ocean subsurface warming significantly increases the rate of mass loss from the ice shelf fronting the HSIS. Our results thus support simplified climate modeling results, suggesting that a weakened or collapsed ice-shelf would trigger an ice-stream surge, producing a Heinrich event (5, 6), analogous to the recent response of Antarctic glaciers to the loss of buttressing ice shelves (34). By confirming the significance that subsurface warming played in triggering past ice-sheet instabilities, our results provide important insights into possible future behavior of similarly configured Antarctic ice-sheet sectors, should warmer waters penetrate beneath their large, buttressing ice shelves.

## Methods

We used an automated flow-through system (35) that cleans and dissolves the carbonate shells and thus minimizes the effects of secondary calcite and clay contamination (*SI Text*). We analyzed the benthic species *C. lobulatus* ($N = 46$), *C. spp.* ($N = 23$), and *M. barleeanum* ($N = 44$), including 15 replicate analyses, and converted Mg/Ca ratios to BWTs following published calibration curves (*SI Text*). The age model for EW9302-2JPC is based on six previously published $^{14}C$ dates (8), well-dated tephra layers at 16- (Vedde Ash) and 408-cm depth (ASH II), an age-to-depth tie point at the midpoint of H6 (36) corresponding to the peak in ice-rafted detrital carbonate at 496-cm depth in EW9302-2JPC, and the marine isotope stage 5/4 boundary (544 cm) based on the $\delta^{18}O$ planktonic foraminifera data from the core (8) (*SI Text*). We emphasize, however, that the relative timing of changes of any given proxy within the core relative to those of another proxy is established directly from the stratigraphic position of each sample within the core and is thus insensitive to any uncertainties in numerical chronology.

**ACKNOWLEDGMENTS.** We thank Ellen Roosen of the Woods Hole Oceanographic Institution core repository for subsampling of EW9302-2JPC, Trond Dokken (Bjerknes Center for Climate Research, Bergen, Norway) for providing samples from MD95-2010, Anne Jennings and Matthew Wolhowe for technical assistance, Tine Rasmussen for sharing data, and Thomas Bauska, Steven Hostetler, Alan Mix, Jeremy Shakun, Joseph Stoner, and two anonymous reviewers for comments. Support was provided by the National Science Foundation Paleoclimate Program (to P.U.C., G.P.K., A.E.C., Z.L., B.O.-B., and A.S.) and National Aeronautics and Space Administration Grant NNG05GR58G (to L.P.). Computer time was provided by the Department of Energy Innovative and Novel Computational Impact on Theory and Experiment program. This is Earth and Space Research contribution number 142.

1. Heinrich H (1988) Origin and consequences of cyclic ice rafting in the Northeast Atlantic ocean during the past 130,000 years. *Quat Res* 29:142–152.
2. MacAyeal DR (1993) Binge/purge oscillations of the Laurentide Ice Sheet as a cause of the North Atlantic's Heinrich events. *Paleoceanography* 8:775–784.
3. Zahn R, et al. (1997) Thermohaline instability in the North Atlantic during meltwater events: Stable isotope and ice-rafted detritus records from core SO75-26KL, Portugues margin. *Paleoceanography* 12:696–710.
4. Clark PU, Hostetler SW, Pisias NG, Schmittner A, Meissner KJ (2007) Mechanisms for an ~7-kyrs climate and sea-level oscillation during Marine Isotope Stage 3. *Ocean Circulation: Mechanisms and Impacts—Past and Future Changes of Meridional Overturning*, eds A Schmittner, JCH Chiang, and SR Hemming (Am Geophysical Union, Washington, DC) p 392.
5. Shaffer G, Olsen SM, Bjerrum CJ (2004) Ocean subsurface warming as a mechanism for coupling Dansgaard-Oeschger climate cycles and ice-rafting events. *Geophys Res Lett* 31:L24202, 10.1029/2004GL020968.
6. Alvarez-Solas J, et al. (2010) Links between ocean temperature and iceberg discharge during Heinrich events. *Nat Geosci* 3:122–126.
7. Alley RB, Anandakrishnan S, Dupont TK, Parizek BR, Pollard D (2007) Effect of sedimentation on ice-sheet grounding-line stability. *Science* 315:1838–1841.
8. Rasmussen TL, Oppo DW, Thomsen E, Lehman SJ (2003) Deep sea records from the southeast Labrador Sea: Ocean circulation changes and ice-rafting events during the last 160,000 years. *Paleoceanography* 18, 10.1029/2001PA000736.
9. Meland MY, Dokken TM, Jansen E, Hevrøy K (2008) Water mass properties and exchange between the Nordic seas and the northern North Atlantic during the period 23-6 ka: Benthic oxygen isotopic evidence. *Paleoceanography* 23:PA1210, 10.1029/2007PA001416.
10. Dokken T, Jansen E (1999) Rapid changes in the mechanism of ocean convection during the last glacial period. *Nature* 401:458–461.
11. Holland DM, Jenkins A (1999) Modelling thermodynamic ice-ocean interactions at the base of an ice shelf. *J Phys Oceanogr* 29:1787–1800.
12. Liu Z, et al. (2009) Transient simulation of last deglaciation with a new mechanism for Bølling-Allerød warming. *Science* 325:310–314.
13. Elderfield H, Yu J, Anand P, Kiefer K, Nyland B (2006) Calibrations for benthic foraminiferal Mg/Ca paleothermometry and the carbonate ion hypothesis. *Earth Planet Sci Lett* 250:633–649.
14. Lewis E, Wallace DWR (1998) CO2 system calculations, ORNL/CDIAC-105 (CO2SYS v.1.05)..
15. WOCE (2002) *World Ocean Circulation Experiment, Global Data, Version 30* (WOCE International Project Office, Southampton, UK).
16. Yu J, Elderfield H, Pitrowski AM (2008) Seawater carbonate ion-$\delta^{13}C$ systematics and application to glacial-interglacial North Atlantic ocean circulation. *Earth Planet Sci Lett* 271:209–220.
17. Adkins JF, McIntyre K, Schrag DP (2002) The salinity, temperature, and $\delta^{18}O$ of the glacial deep ocean. *Science* 298:1769–1773.
18. O'Neil JR, Clayton RN, Mayeda TK (1969) Oxygen isotope fractionation in divalent metal carbonates. *J Chem Phys* 51:5547–5558.
19. McManus JF, Francois R, Gherardi J-M, Keigwin LD, Brown-Leger S (2004) Collapse and rapid resumption of Atlantic meridional circulation linked to deglacial climate changes. *Nature* 428:834–837.
20. Mangini A, et al. (2010) Deep sea corals off Brazil verify a poorly ventilated Southern Pacific Ocean during H2, H1 and the Younger Dryas. *Earth Planet Sci Lett* 293:269–276.
21. Bond G, Lotti R (1995) Iceberg discharges into the North Atlantic on millennial time scales during the last deglaciation. *Science* 267:1005–1010.
22. Gutjahr M, Hoogakker BAA, Frank M, McCave IN (2010) Changes in North Atlantic Deep Water strength and bottom water masses during Marine Isotope Stage 3 (45–35 ka BP). *Quat Sci Rev* 29:2451–2461.
23. Clark PU, McCabe AM, Mix AC, Weaver AJ (2004) Rapid rise of sea level 19,000 years ago and its global implications. *Science* 304:1141–1144.
24. Ruhlemann C, Mulitza S, Muller PJ, Wefer G, Zahn R (1999) Warming of the tropical Atlantic Ocean and slowdown of thermohaline circulation during the last deglaciation. *Nature* 402:511–514.
25. Rasmussen TL, Thomsen E, van Weering TCE, Labeyrie L (1996) Rapid changes in surface and deep water conditions at the Faeroe Margin during the last 58,000 years. *Paleoceanography* 11:757–772.
26. Rasmussen TL, Thomsen E (2004) The role of the North Atlantic Drift in the millennial timescale glacial climate fluctuations. *Paleogeogr Paleoclimatol Paleoecol* 210:101–116.
27. Bond G, et al. (1993) Correlations between climate records from North Atlantic sediments and Greenland ice. *Nature* 365:143–147.
28. Blunier T, Brook EJ (2001) Timing of millennial-scale climate change in Antarctica and Greenland during the last glacial period. *Science* 291:109–112.
29. Crowley TJ (1992) North Atlantic deep water cools the southern hemisphere. *Paleoceanography* 7:489–497.
30. Robinson LF, et al. (2005) Radiocarbon variability in the western North Atlantic during the last deglaciation. *Science* 310:1469–1473.
31. Hulbe CL (1997) An ice shelf mechanism for Heinrich layer production. *Paleoceanography* 12:711–717.
32. Rignot E, Jacobs SS (2002) Rapid bottom melting widespread near Antarctic Ice Sheet grounding lines. *Science* 296:2020–2023.

33. Joughin I, Smith BE, Holland DM (2010) Sensitivity of 21st century sea level to ocean-induced thinning of Pine Island Glacier, Antarctica. *Geophys Res Lett* 37:L20502, 10 .1029/2010GL044819.
34. Rignot E, et al. (2004) Accelerated ice discharge from the Antarctic Peninsula following the collapse of Larsen B ice shelf. *Geophys Res Lett* 31:L18401, 10.1029/2004GL020697.
35. Haley BA, Klinkhammer GP (2002) Development of a flow-though system for cleaning and dissolving foraminiferal tests. *Chem Geol* 185:51–69.
36. Stoner JS, Channell JET, Hillaire-Marcel C, Kissel C (2000) Geomagnetic paleointensity and environmental record from Labrador Sea core MD95-2024: Global marine sediment and ice core chronostratigraphy for the last 110 kyr. *Earth Planet Sci Lett* 183:161–177.
37. Jouzel J, et al. (2007) Orbital and millennial Antarctic climate variability over the past 800,000 years. *Science* 317:793–796.
38. Lemieux-Dudon B, et al. (2010) Consistent dating for Antarctic and Greenland ice cores. *Quat Sci Rev* 29:8–20.
39. NGRIP members (2004) High-resolution record of Northern Hemisphere climate extending into the last interglacial period. *Nature* 431:147–151.
40. Meese DA (1997) The Greenland Ice Sheet Project 2 depth-age scale: Methods and results. *J Geophys Res* 102:26411–26423.
41. Rühlemann C, et al. (2004) Intermediate depth warming in the tropical Atlantic related to weakened thermohaline circulation: Combining paleoclimate data and modeling results for the last deglaciation. *Paleoceanography* 19, 10.1029/2003PA000948.